

Theoretical Study of Ethynylbenzene Adsorption on Au(111) and Implications for a New Class of Self-Assembled Monolayer

M. J. Ford,* R. C. Hoft, and A. McDonagh

Institute for Nanoscale Technology, University of Technology Sydney, P.O. Box 123, Broadway, NSW 2007, Australia

Received: June 16, 2005; In Final Form: August 30, 2005

Density functional calculations of the adsorption of ethynylbenzene on the Au(111) surface show that, after cleavage of the C–H bond, the terminal carbon makes a strong covalent bond to the surface. The bond energy is shown to be about 70 kcal·mol^{−1} with the fcc hollow site being most stable and the molecule oriented perpendicular to the surface. Adsorption without elimination of hydrogen is also possible via a hydrogen 1,2 shift to form a vinylidene surface-bound species, or opening of the C–C triple bond and adsorption through the two carbon atoms in a flat conformation. The reaction energy for formation of the surface-bound vinylidene is estimated to be 5 kcal·mol^{−1} exothermic relative to the isolated ethynylbenzene and gold substrate.

1. Introduction

Self-assembled monolayers (SAMs) have taken a central role in nanoscience and technology. They are generally easy to prepare on a range of surfaces more or less independent of size and shape. General reviews of the field have been published by Ulman.^{1,2} Perhaps the most widely used SAMs are thiolates on gold surfaces. Thiols form relatively strong bonds to the surface atoms, and can be sufficiently mobile to allow ordering of the overlayer. Love et al. have recently published a thorough review of thiolate SAMs and their applications.³ Moreover, thiol “alligator clips” are commonly used to anchor molecules to metal surfaces in measurements of electron transport properties.^{4–6}

Metal–alkyne complexes are well-known in organometallic chemistry.⁷ Anchoring a molecule via an alkynyl group should provide an unbroken π -conjugated linkage to the gold surface. This has considerable promise in the study of transport properties and may provide insight to unresolved questions involving electron conduction in molecular wires. Furthermore, a wide range of terminal alkynes are synthetically accessible that may be suitable for SAM formation.

In this paper, we present the first computational study of the interaction of a terminal alkyne with the bulk Au(111) surface. We choose a simple representative molecule, ethynylbenzene (Figure 1), to explore the adsorption energetics and potential pathways for forming monolayers. Previous experimental studies using surface-enhanced Raman spectroscopy have shown that the ethynylbenzene binds to gold surfaces⁸ and nanoparticles,⁹ but these studies are inconclusive about the nature of the gold–alkyne bond.

2. Method

Calculations were performed using the SIESTA software package.^{10,11} This is a density functional, pseudopotential code with periodic boundary conditions. Atom-centered basis sets describe the valence electrons. We have used the counterpoise method of Boys and Bernadi¹² to correct for basis set superposi-

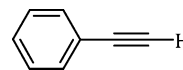


Figure 1. Ethynylbenzene.

tion errors (BSSE). Such methods do not always provide improved interaction energies;¹³ however, for modest sized basis sets and strong interactions it is expected to give reasonable results.

The generalized-gradient approximation (GGA) to the exchange–correlation functional due to Perdew, Burke, and Ernzerhof (PBE)¹⁴ is used throughout. All calculations are spin unrestricted and employ a Fermi smearing of 25 meV to aid convergence. Core electrons are represented by norm-conserving pseudopotentials¹⁵ (with a relativistic correction in the case of Au), and valence electrons by double- ζ plus single polarization basis sets.

Transferability of the pseudopotentials has been demonstrated previously.^{16–18} The carbon and hydrogen pseudopotentials have also been checked by comparing with all electron calculations at the same level of theory drawn from the Computational Chemistry Comparison and Benchmark database¹⁹ and calculated with the Gaussian package²⁰ (see Supporting Information section S1).

The gold substrate is modeled using a multilayer slab (3, 4, or 7 layers) with 3 \times 3 atoms in each layer. The lattice parameter is from an optimization of bulk gold performed at the same computational level. The intermolecular spacing is greater than 0.5 nm with negligible intermolecular interaction; in other words, we are simulating single molecule adsorption.

Calculations have been performed stepwise at increasing levels of accuracy (see Supporting Information section S2). Survey calculations where a rigid molecule is scanned at fixed height across a rigid 3 layer slab allow the adsorption sites to be identified. Full geometry optimizations of the molecule, and subsequent optimizations of the molecule and surface layer of the slab, were then performed for the adsorption sites on a 4 layer slab at an intermediate level. Final energies are then calculated at a high level without further optimization on a 7 layer slab. With respect to the computational parameters and

* To whom correspondence should be addressed. E-mail: Mike.Ford@uts.edu.au.

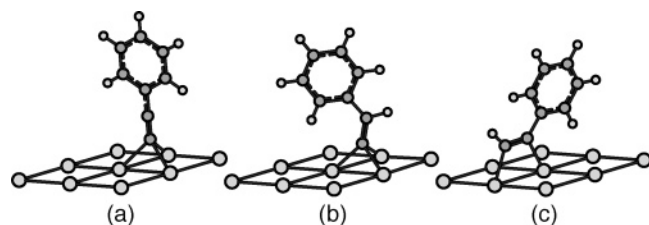


Figure 2. Configuration of surface-bound molecule: (a) final state, (b) vinylidene intermediate, and (c) flat intermediate.

the 7 layer slab used in the high level calculations, interaction energies are converged to better than $1 \text{ kcal}\cdot\text{mol}^{-1}$.

A small number of Gaussian calculations were carried out using the PBE correlation-exchange functional and 6-31G** basis sets on all but the Au atoms where a LanL2DZ basis was used. In the case of adsorbed species, the gold surface was represented by a cluster of 9 atoms in the surface layer and 4 or 5 atoms in the second layer. Optimized geometries from the SIESTA calculations were used with no reoptimization. In all other instances, structures were geometry optimized in Gaussian.

3. Results and Discussion

In this paper, we consider adsorption processes where the product is a surface-bound molecule in the configuration shown in Figure 2a, where the terminal hydrogen (or proton) has been eliminated. There are a number of possible routes that can lead to this final product. The most direct is homo- or heterolytic cleavage of the C–H bond followed by adsorption of the radical or anion. Intermediate surface bound states are also possible. Reactions of metals with ethynylbenzene can proceed via a 1,2 hydrogen shift to form metal vinylidenes.²¹ The configuration of the corresponding surface-bound vinylidene is shown in Figure 2b. The third possibility is via a π -interaction through both carbon atoms to give the flat geometry shown in Figure 2c. The reaction could then proceed by C–H bond cleavage (or deprotonation) to give the product shown in Figure 2a.

3.1. Single Molecule–Surface Interaction Energies. We first discuss the energetics and nature of the interaction for the configuration in Figure 2a, and we will return to the issue of pathways and the intermediate states later. The results of the constant height survey scan of the rigid ethynylbenzene radical over the Au(111) surface are shown in Figure 3a. The position of the contour plot relative to the surface atoms is shown in Figure 3b. The two hollow sites differ: the hcp site has a second layer Au atom directly below it whereas the fcc site does not. The latter has a third layer atom directly below.

The potential energy surface is relatively flat; a line joining the hcp–bridge–fcc sites varies in energy by approximately $5 \text{ kcal}\cdot\text{mol}^{-1}$. Figure 3 suggests that hcp and fcc are the most likely binding sites. However, the bridge and atop sites cannot be ruled out entirely. Consequently, structure optimizations were performed starting from all four sites.

Interaction energies for the four sites are given in Table 1. Interactions are calculated from the energy of the entire system minus the energies of the two components in the adsorbed geometries and are BSSE corrected.

An interaction energy of $\sim 69 \text{ kcal}\cdot\text{mol}^{-1}$ indicates that the ethynylbenzene radical is strongly bound to the gold surface. For comparison, we have performed similar level calculations for phenylenedimethanethiol adsorption on gold where the interaction is closer to $35 \text{ kcal}\cdot\text{mol}^{-1}$. Our earlier calculations of methanethiol¹⁸ adsorption on gold using the same methods also give adsorption energies of around $30 \text{ kcal}\cdot\text{mol}^{-1}$. The current results are consistent with our calculations for an

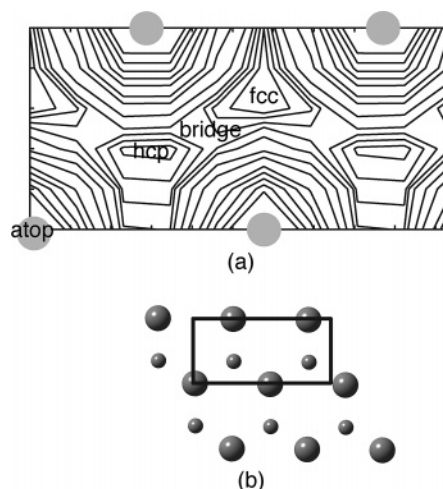


Figure 3. (a) Contour plot of the potential energy for the ethynylbenzene radical scanned over the Au(111) surface at a constant height of 1.5 Å . Circles represent positions of surface layer atoms. The hcp and fcc sites are lowest in energy, and atop is highest. (b) Larger section of Au(111) surface. The rectangle shows position of contour plot, and smaller circles are second layer atoms.

TABLE 1: Energies of Interaction between the Ethynylbenzene Radical and Au(111)^a

site	height (Å)	interaction energy ($\text{kcal}\cdot\text{mol}^{-1}$)		
		I	II	III
fcc	1.32	−64.3	−70.3	−68.9
hcp	1.39	−63.7	−67.9	−66.9
bridge		−62.7		
atop	2.01	−57.7	−58.6	−61.9

^a (I) Energies calculated at intermediate level with molecule optimization, (II) intermediate level with molecule + surface layer optimization, and (III) final level. Heights are from the final level calculation for the C atom above the plane of surface Au atoms.

ethynylbenzene–gold–phosphine complex and a phenylenedimethanethiol–gold–phosphine complex, where the Au–C and Au–S interactions energies are 109.8 and $72.7 \text{ kcal}\cdot\text{mol}^{-1}$ respectively. The larger interaction energy of ethynylbenzene compared to similar thiols may therefore be attributed to the stronger Au–C bond compared to the Au–S bond.

The fcc hollow site is marginally the most favorable at all levels, and the atop is least favorable. Allowing the surface layer as well as the molecule to relax (II in Table 1) increases the interaction energies by between 1 and $6 \text{ kcal}\cdot\text{mol}^{-1}$. The change in atomic coordinates of the surface layer atoms is relatively small upon relaxation, with bond lengths changing by about 5% or less. For the bridge site, allowing the surface layer to relax results in the molecule migrating to the fcc site. This is an interesting result that demonstrates surface relaxations, although small, can have quite profound effects. Increasing the computational tolerance and slab thickness to 7 layers (III in Table 1) decreases interaction energies for the hollow sites by about $1 \text{ kcal}\cdot\text{mol}^{-1}$, but increases it for the atop site by about $3 \text{ kcal}\cdot\text{mol}^{-1}$.

The single largest source of error in these calculations is BSSE. The uncorrected energies are 10% larger than those in Table 1.

For all four sites, the radical stands perpendicular to the surface in the optimized geometry. This geometry is, however, a shallow minimum in the total energy curve with respect to tilting the radical relative to the surface as can be seen in Figure 4. In this figure, the total energy is plotted as the entire radical is rotated about the terminal carbon atom from a perpendicular

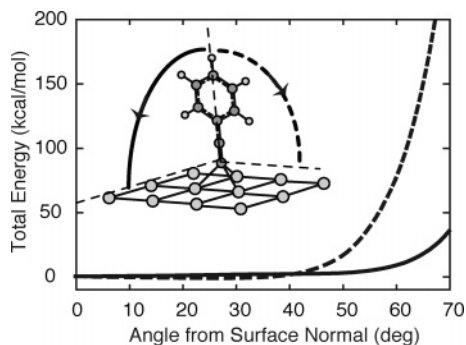
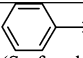
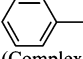
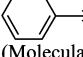


Figure 4. Total energy of ethynylbenzene radical adsorbed at fcc site as a function of tilt angle of radical relative to surface normal. Solid line is ring parallel to surface, and dashed line is ring perpendicular. Inset indicates how the radical is rotated for each curve.

TABLE 2: Comparison of Bond Lengths and Mulliken Charges and Overlap Populations for the Ethynylbenzene Radical Adsorbed in the fcc Site, $\text{PH}_3\text{-Au-Ethynylbenzene}$ Complex, and Ethynylbenzene Molecule

	Bond length (Å)			Mulliken -C≡C-C ₆ H ₅	Overlap
	C≡C	C-Au	C-H		
 (Surface bound)	1.28	2.23 2.24 2.20		-0.10	0.12 0.12 0.15
 (Complex)	1.25 (1.172) ^a	1.98 (2.034) ^a		-0.56	0.07
 (Molecular)	1.24		1.09	-0.17	0.35

^a Experimentally determined (crystal X-ray diffraction data from $\text{C}_6\text{H}_5\text{CC-Au-PMe}_3^{22}$).

orientation to one where it is lying flat on the surface. In one case, the radical is rotated so that the phenyl ring becomes flat on the surface, and in the other, it ends up perpendicular to the surface. The geometry of the radical itself and distance of terminal carbon above the surface are held fixed during the rotation. The total energy does not change by more than 2 $\text{kcal}\cdot\text{mol}^{-1}$ until the tilt angle reaches 50°.

To characterize the nature of the bond in the adsorbed radical, a comparison is made with the gas-phase ethynylbenzene molecule and the $\text{PH}_3\text{-Au-ethynylbenzene}$ complex. The terminal C-H bond in ethynylbenzene is expected to be quite covalent. Bond lengths and Mulliken populations for surface-bound ethynylbenzene in the fcc site, ethynylbenzene, and the $\text{PH}_3\text{-Au-ethynylbenzene}$ complex have been calculated and are given in Table 2. For the surface-bound species, three values are given for the C-Au bond and overlaps corresponding to the three bonds with the nearest surface Au atoms. Overlap populations with all other gold atoms are negligible in this case.

The calculated C≡C and C-Au bond lengths for the gold complex agree to within about 5% with experimental values determined by X-ray crystallography.²² The C≡C bond length is similar in all three cases. The decrease in C-Au (C-H for the molecule) bond length across the table is perhaps misleading as the height of the surface-bound species above the gold surface is only 1.32 Å. From the bond lengths, it is difficult to determine any difference in the bonds of the three species. The Mulliken charges of the -C≡C-phenyl fragment and overlap populations are more conclusive and indicate that the surface-bound species forms a covalent bond with the surface. The Mulliken charge is relatively small, and total overlap population with the three surface gold atoms is relatively large. This is also the case for

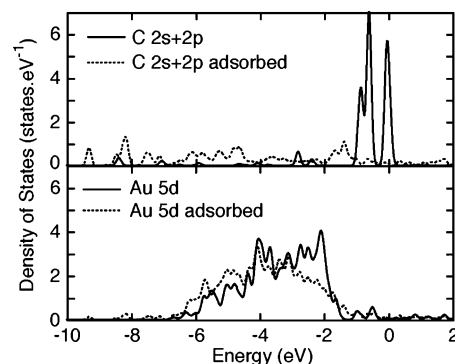


Figure 5. Orbital projected densities of states for the carbon atom on the radical and one surface Au atom involved in the bond, before adsorption (solid lines) and after adsorption (dashed lines). Energies are relative to the Fermi energy.

the C-H bond in the molecule, whereas the complex shows a more polar bond.

Changes in the density of states for the radical and Au slab in isolation compared with the adsorbed radical can provide information on which orbitals are participating in the bond. The densities of states projected onto the 2s + 2p orbitals of the bonding carbon atom on the radical and onto the 5d orbital of a surface Au atom involved in the bond are shown in Figure 5. Integrating these densities below the Fermi level gives the expected number of electrons both before and after adsorption; a total of 4 in the C-based orbitals and 10 in the Au 5d orbitals. The C-2sp orbital near the Fermi level becomes very diffuse upon adsorption, and the Au-5d orbitals shift to lower energy. Densities projected onto other orbitals (i.e., Au 6s and 6p) show very little change upon adsorption. From this, it can be inferred that the 2sp carbon orbital mixes with the metal 5d orbitals to form a hybrid which stabilizes the bond, i.e., a bonding orbital lying lower in energy.

Substituent effects on the interaction energy have also been calculated. Upon substitution of the hydrogen in the 4-position of the benzene ring with either an electron-withdrawing NO_2 group (1-ethynyl-4-nitrobenzene) or an additional ethynyl group (1,4-diethynylbenzene), almost identical interaction energies are observed, being about 2 $\text{kcal}\cdot\text{mol}^{-1}$ larger for the NO_2 substituent and about 2 $\text{kcal}\cdot\text{mol}^{-1}$ smaller for the ethynyl substituent compared to ethynylbenzene.

3.2. Intermediate Surface States and Reaction Pathways.

We now return to the question of the possible intermediate surface bound states shown in Figure 2b,c, and estimate overall reaction energies.

The potential energy surface of the vinylidene configuration, determined by survey scans across the Au(111) surface, is similar to the results in section 3.1, with fcc, hcp, bridge, and atop adsorption sites. Survey scans of the flat adsorption geometry also reveal a relatively flat potential energy surface corrugated by about 3.5 $\text{kcal}\cdot\text{mol}^{-1}$. The minimum occurs with the two adsorbing carbon atoms positioned above two surface atoms, as shown in Figure 2c. Geometry optimizations from a number of starting configurations all converge to this same optimum geometry. Interaction energies calculated in the same manner as detailed in section 3.1 are given in Table 3.

The molecule/radical forms a strong bond to the surface in all three configurations. This is in contrast to thiol molecules where the interaction is weaker if the terminal hydrogen is not removed.²³ Previous surface-enhanced Raman (SERS) experiments suggest the possibility that ethynylbenzene can adsorb onto a gold surface in the flat geometry;⁸ this point is discussed in more detail below.

TABLE 3: Interaction Energies Calculated at the Final Level for the Vinylidene and Flat Molecule Configurations^a

	site	energy (kcal·mol ⁻¹)	
		interaction	overall
vinylidene	fcc	-56.4	-5.6
	hcp	-52.2	
	bridge		
	atop	-28.9	
flat geometry	atop	-42.5	0.7
ethynylbenzene	fcc	-68.9	58.6

^a Interaction energy of the ethynylbenzene radical from Table 2 is also included. Overall energies are energies of the surface-bound species relative to the relaxed, isolated molecule and slab.

For the π -bound molecule in the flat geometry, the two bonded carbon atoms are 1.94 and 1.98 Å above the plane of the surface atoms, and the Au–C bond lengths are 2.13 and 2.10 Å. The bond is predominantly between a single carbon atom and a single surface gold atom. Mulliken overlap populations between each of the carbon atoms and nearest surface gold atom are 0.34 and 0.35. The surface bond again displays a strong covalent character.

The atop site for the vinylidene configuration is considerably less favorable, presumably because the molecule makes an sp^2 bond to the surface. Once again, the bridge site is a saddle point, with the molecule optimizing to the fcc hollow. Unlike ethynylbenzene, the vinylidene bound at the bridge site is unstable irrespective of whether the surface layer of gold atoms is relaxed. Adsorption heights are less than 5% shorter than ethynylbenzene. There are significant Mulliken overlap populations between the carbon atom and three surface gold atoms (0.16, 0.19, and 0.15). From the data presented above, we suggest that the vinylidene and ethynylbenzene should interact in a similar manner with the gold surface.

The overall energies given in Table 3 are energies of the surface-bound molecule/radical relative to the energies of the isolated molecule plus gold slab in their relaxed geometries. Importantly, despite the large geometry change, the overall reaction energy from a gas phase ethynylbenzene molecule plus gold slab to a surface-bound species is energetically favorable for the vinylidene configuration (5.6 kcal·mol⁻¹ exothermic) and only marginally unfavorable for the flat geometry (0.7 kcal·mol⁻¹ endothermic).

The ethynylbenzene case is obviously very endothermic (58.6 kcal·mol⁻¹) because it involves cleavage of the C–H bond prior to adsorption. We calculate the latter energy to be 126.5 kcal·mol⁻¹. Peterson and Dunning²⁴ in their calculations using correlation consistent basis sets quote an experimental value for the C–H bond energy in acetylene of 139.3 kcal·mol⁻¹. Their calculated values at the Hartree–Fock level are around 117 kcal·mol⁻¹, while large multiconfiguration calculations are required to approach the experimental value. In our calculations, employing pseudopotentials, we might expect bonds involving hydrogen atoms, which have small bond lengths, to be problematic despite our care in ensuring the pseudopotential cutoff radii are appropriate. We expect this problem not to be so troublesome with the longer C–Au bonds calculated in this work.

Formation of the surface-bound radical could proceed via deprotonation as well as homolytic C–H bond cleavage. The former is unlikely for direct adsorption since the pK_a for this molecule is around 30. However, metal complexes with ethynylbenzene can be prepared through deprotonation of the corresponding vinylidene,²¹ and examples of ruthenium and osmium vinylidene complexes have been isolated.²¹ Conse-

TABLE 4: Reaction Energies for Reactions 1 and 2 and C–H Bond and Deprotonation Energies^a

pathway	energy (kcal·mol ⁻¹)			
	C–H	reaction 1	deprot	reaction 2
vinylidene	84.0	13.4	321.6	39.5
flat geometry	80.1	16.2	316.7	42.1
ethynylbenzene	126.5	8.2	369.7	39.4

^a Reaction 2 includes the proton solvation energy in water.

quently, energies for reactions 1 and 2 below via direct adsorption and the two intermediate surface-bound states have been calculated and are given in Table 4.



Our calculated value for the H–H bond energy is 98 kcal·mol⁻¹, and the all-electron value at the same level is 104.2 kcal·mol⁻¹.¹⁹ Calculated values for the C–H bond energy and deprotonation energies for the molecule and two surface-bound intermediates are also given in Table 4.

In reaction 2, the adsorbate–substrate has been assigned a formal charge of -1. The fate of the electron, after deprotonation is not immediately apparent. In solution, any charge would be compensated by the counterions present (for example, gold nanoparticles in solution can be stabilized by a negative charge imparted by adsorbed citrate ions^{25,26}).

The energies shown in this table are rather approximate for reasons described above. However, the trend in the calculated C–H bond energies for ethynylbenzene and the vinylidene is consistent with the trend in experimental C–H bond energies for acetylene (139.3 kcal·mol⁻¹) and the vinylidene isomer of acetylene, ethynylidene (89.7 kcal·mol⁻¹).²⁴

Reaction energies for reactions 1 and 2 should be the same independent of the intermediate pathway. Reaction energies for the C–H bond cleavage reaction (reaction 1) are all slightly endothermic and range over 8 kcal·mol⁻¹. Given the difficulty of calculating the C–H and H–H bond energies and the fact that errors are likely to build up in calculating the various steps in the reaction, a reliability of 8 kcal·mol⁻¹ is reasonable.

The deprotonation reaction energies (reaction 2) agree far better. The reliability in this case seems to be about 3 kcal·mol⁻¹, and the reaction is quite endothermic. The energy gain from solvation of the proton in water is included in these values in order to give an indication of the likely overall reaction energy. We use a value of 262.4 kcal·mol⁻¹ taken from the computational literature.²⁷ In practice, other solvents are more likely to be used, and it would be instructive to compare reaction energies in various solvents or the effects of pH. However, reliable values of the proton solvation energies in solvents other than water are not readily available in the literature, and calculating these values is beyond the scope of the present work. Tuttle et al.²⁸ give a preliminary estimate for the proton solvation energy in ammonia of about 287 kcal·mol⁻¹, giving an overall energy for reaction 2 of about 15 kcal·mol⁻¹. In the appropriate solvent, the deprotonation pathway (reaction 2) may become energetically favorable.

Previous surface enhanced Raman studies (SERS) of ethynylbenzene on gold nanoparticles⁹ and surfaces⁸ are somewhat inconclusive and depend on the nature of the enhancement mechanism. Multiple peaks ascribed to the C≡C stretch are observed in the region of 2000 cm⁻¹, and there is a broad and intense band due to the C=C bond around 1600 cm⁻¹. These

observations do not determine unambiguously the orientation of the molecules on the surface, but they do indicate that several species are present. Our calculations support this conclusion and show that it may indeed be possible to have coexistence of sp and sp^2 hybridized species on the surface. It is interesting to note that the SERS study with gold surfaces⁸ indicates adsorption in a flat configuration while the nanoparticle study⁹ suggests an upright configuration. A possible explanation for this result is that in the former case the intermediate state in Figure 2c dominates, while in the latter case addition of a base (in preparing the gold nanoparticles) has driven the reaction to the final upright configuration of Figure 2a.

4. SAM Formation

We do not address the question of SAM formation through direct calculation as this requires a model that can predict dispersion forces. However, insights based upon the results of the calculations presented above, together with work by others, can be used to assess the potential of ethynylbenzene to form SAMs.

SAM formation depends sensitively on the balance between headgroup–substrate interaction and tail–tail interactions. The molecule must be bound to the surface yet sufficiently mobile to self-assemble under the driving force of the tail–tail interactions. The assembling force for ethynylbenzene will be interactions between the phenyl rings.²⁹ This is a dispersive force with an intermolecular strength between pairs of benzene molecules of about $2.5 \text{ kcal}\cdot\text{mol}^{-1}$. There are two possible orientations: offset-face-to-face (OFF) where the phenyl rings are parallel but offset slightly, or edge-to-face (EF). The plane separation for the OFF motif is generally about 3.5 \AA , and the offset is about 1.8 \AA . The centroid–centroid separation for the EF motif is 5 \AA .

Despite the strength of the interaction with gold, the ethynylbenzene radical is quite mobile along the hcp–bridge–fcc path (see Figure 2), with a diffusion barrier of only a few kilocalories per mole. Similar diffusion paths and barriers have been found for thiol radicals on Au(111).²³ Hence, it might be expected that the interactions between the tail groups of ethynylbenzene are sufficient to drive self-assembly and that the most likely structure to form is the same as the analogous thiol SAM.

The most commonly reported overlayer structure for thiol-bound molecules absorbed on Au(111) is $\sqrt{3}\times\sqrt{3}R30$ where the intermolecular spacing is 4.97 \AA .^{2,3} The short ethynylbenzene molecule cannot pack in this structure and optimize the interactions in the OFF configuration. Longer molecules can tilt relative to the surface to reduce the tail–tail distance. By forming a herringbone pattern in the $\sqrt{3}\times\sqrt{3}R30$ configuration as shown in Figure 6, molecules upright on the surface will be at the optimum distance for the EF configuration. This overlayer structure has also been suggested for aromatic thiol SAMs on gold surfaces.³⁰ Each molecule interacts edge-to-face with four of its nearest neighbors giving a total interaction of approximately $5 \text{ kcal}\cdot\text{mol}^{-1}$. This is the same order of magnitude as our estimate of the barrier to surface diffusion along the fcc–bridge–hcp path. An X-ray crystallographic study of ethynylbenzenes found that EF interactions were present in the molecular crystal of ethynylbenzene but not 1,4-diethynylbenzene or 1,3,5-triethynylbenzene.³¹ The latter two are dominated by hydrogen bonding between the ethynyl hydrogen atoms and π -electrons of the triple bond.

A feasible mechanism of monolayer formation, based upon the calculations presented here, is through the vinylidene

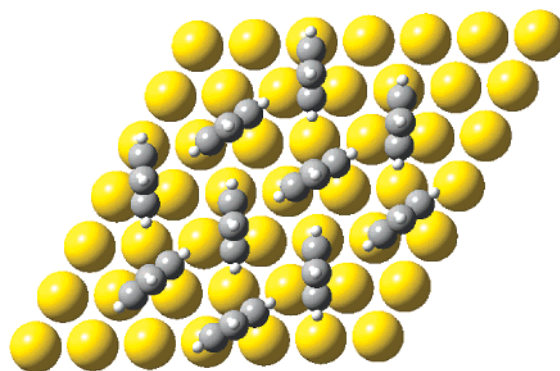


Figure 6. Herringbone $\sqrt{3}\times\sqrt{3}R30$ overlayer structure.

surface-bound intermediate, since this reaction is overall exothermic. Elimination of the hydrogen atom through formation of H_2 gives an endothermic reaction energy overall, on the order of $10 \text{ kcal}\cdot\text{mol}^{-1}$. Surface adsorption of the free hydrogen is also possible. Although our calculations estimate that deprotonation to yield the final surface-bound ethynylbenzene is overall strongly endothermic, in a basic environment this pathway is also feasible. In fact, many metal–ethynylbenzene complexes are synthesized through this mechanism.^{21,22} A more detailed study of the reaction mechanism would require identifying transition states and hence barriers to the various pathways. This is outside the scope of the present work and is a difficult task using the current computational methods.

5. Conclusions

Density functional calculations using the generalized gradient approximation for single molecule adsorption of the ethynylbenzene radical on the Au(111) surface show that a strong covalent bond is formed with the surface upon removal of the terminal hydrogen (or deprotonation). The fcc hollow site is most energetically favorable with an interaction energy of $68.9 \text{ kcal}\cdot\text{mol}^{-1}$. The radical is adsorbed perpendicular to the surface through the terminal carbon.

The molecule can also undergo a hydrogen 1,2 shift and form a vinylidene surface-bound species, or adsorb flat on the surface by opening the triple bond and bonding through the two carbon atoms. The former reaction is overall exothermic by $5.6 \text{ kcal}\cdot\text{mol}^{-1}$. The latter is calculated to be marginally endothermic by $0.7 \text{ kcal}\cdot\text{mol}^{-1}$, although this energy is likely to be below the overall reliability of the present calculations.

The overall reaction energy for formation of a surface-bound ethynylbenzene radical and hydrogen molecules from the isolated molecule is estimated to be on the order of $10 \text{ kcal}\cdot\text{mol}^{-1}$ endothermic. By using the accepted value for the proton solvation energy in water, we estimate the reaction energy via deprotonation is to be on the order of $40 \text{ kcal}\cdot\text{mol}^{-1}$.

The barrier to surface diffusion of the ethynylbenzene radical, estimated to be $5 \text{ kcal}\cdot\text{mol}^{-1}$, is similar to the expected interaction energy between the molecular tail groups indicating that self-organization of the adsorbed molecules is likely.

These calculations demonstrate that compounds incorporating the ethynylbenzene moiety offer a promising alternative to thiol compounds for anchoring organic molecules to gold surfaces to form self-assembled monolayers. This linking scheme would have the advantage of being more oxidatively stable, offering improved long-term stability of the SAM. Monolayers of double-ended molecules could also be formed without the problems of multiple layer formation associated with dithiol SAMs, particularly aromatic dithiols. In addition, by eliminating the sulfur atom, conjugation to the gold surface is unbroken.

We suggest that experimental preparation procedures should be tried both with and without the inclusion of a base. Although the 1,2 hydrogen shift to yield a vinylidene surface-bound intermediate is a promising candidate pathway, these calculations do not unambiguously determine whether subsequent C–H bond cleavage or deprotonation is more likely. The latter is, however, known to be the case in the synthesis of metal complexes of ethynylbenzene. In any case, it is likely that heating of the solution is required due to the predicted endothermicity of the overall reaction. If indeed a SAM is formed, the molecules are likely to be adsorbed perpendicular to the surface giving a monolayer thickness of 8 Å. The surface structure is likely to be a $\sqrt{3}\times\sqrt{3}$ R30 overlayer with the molecules forming a herringbone pattern. Molecules with additional phenyl rings should also be investigated in order to increase the tail–tail interaction that drives self-assembly.

Acknowledgment. This work was supported by the Australian Research Council and the University of Technology, Sydney. A. McDonagh holds an Australian Research Council Postdoctoral Fellowship. Computational resources were provided under the merit allocation schemes of the Australian Centre for Advanced Computing in New South Wales and the National Facility at the Australian Partnership for Advanced Computing.

Supporting Information Available: Details of pseudopotential validation and computational parameters. This material is available free of charge via the Internet at <http://pubs.acs.org>.

References and Notes

- (1) Ulman, A. *An Introduction to Ultrathin Organic Films*; Academic Press: Boston, 1991.
- (2) Ulman, A. *Chem. Rev.* **1996**, *96*, 1533.
- (3) Love, J. C.; Estroff, L. A.; Kriebel, J. K.; Nuzzo, G.; Whitesides, G. M. *Chem. Rev.* **2005**, *105*, 1103.
- (4) Nitzan, A.; Ratner, M. A. *Science* **2003**, *300*, 1384.
- (5) McCreery, R. L. *Chem. Mater.* **2004**, *16*, 4477.
- (6) James, D. K.; Tour, J. M. *Chem. Mater.* **2004**, *16*, 4423.
- (7) Long, N. J.; Williams, C. K. *Angew. Chem.* **2003**, *42*, 2586.
- (8) Feilchenfeld, H.; Weaver, M. J. *J. Phys. Chem.* **1989**, *93*, 4276.
- (9) Joo, S.-W.; Kim, K. *J. Raman Spectrosc.* **2004**, *35*, 549.
- (10) Ordejon, P.; Artacho, E.; Soler, J. M. *Phys. Rev. B: Condens. Matter* **1996**, *53*, R10441.
- (11) Soler, J. M.; Artacho, E.; Gale, J. D.; Garcia, A.; Junquera, J.; Ordejon, P. *J. Phys.: Condens. Matter* **2002**, *14*, 2745.
- (12) Boys, S. B.; Bernardi, F. *Mol. Phys.* **1970**, *19*, 533.
- (13) Lampropoulos, N. A.; Reimers, J. R. *J. Chem. Phys.* **2002**, *116*, 10277.
- (14) Perdew, J. P.; Burke, K.; Ernzerhof, M. *Phys. Rev. Lett.* **1996**, *77*, 3865.
- (15) Troullier, N.; Martins, J. L. *Phys. Rev. B* **1991**, *43*, 1993.
- (16) Masens, C. Density functional theory assessment of self-assembled monolayers on gold surfaces. Ph.D. Dissertation, University of Technology, Sydney, 2004.
- (17) Soule de Bas, B.; Ford, M. J.; Cortie, M. B. *THEOCHEM* **2004**, *686*, 193.
- (18) Masens, C.; Ford, M. J.; Cortie, M. B. *Surf. Sci.* **2005**, *580*, 19.
- (19) PBE/6-31G* all electron calculations taken from the NIST Computational Chemistry Comparison and Benchmark Database (CCCBDB) at srdata.nist.gov.
- (20) Frisch, M. J.; Trucks, G. W.; Schlegel, H. B.; Scuseria, G. E.; Robb, M. A.; Cheeseman, J. R.; Montgomery, J. A., Jr.; Vreven, T.; Kudin, K. N.; Burant, J. C.; Millam, J. M.; Iyengar, S. S.; Tomasi, J.; Barone, V.; Mennucci, B.; Cossi, M.; Scalmani, G.; Rega, N.; Petersson, G. A.; Nakatsuji, H.; Hada, M.; Ehara, M.; Toyota, K.; Fukuda, R.; Hasegawa, J.; Ishida, M.; Nakajima, T.; Honda, Y.; Kitao, O.; Nakai, H.; Klene, M.; Li, X.; Knox, J. E.; Hratchian, H. P.; Cross, J. B.; Bakken, V.; Adamo, C.; Jaramillo, J.; Gomperts, R.; Stratmann, R. E.; Yazyev, O.; Austin, A. J.; Cammi, R.; Pomelli, C.; Ochterski, J. W.; Ayala, P. Y.; Morokuma, K.; Voth, G. A.; Salvador, P.; Dannenberg, J. J.; Zakrzewski, V. G.; Dapprich, S.; Daniels, A. D.; Strain, M. C.; Farkas, O.; Malick, D. K.; Rabuck, A. D.; Raghavachari, K.; Foresman, J. B.; Ortiz, J. V.; Cui, Q.; Baboul, A. G.; Clifford, S.; Cioslowski, J.; Stefanov, B. B.; Liu, G.; Liashenko, A.; Piskorz, P.; Komaromi, I.; Martin, R. L.; Fox, D. J.; Keith, T.; Al-Laham, M. A.; Peng, C. Y.; Nanayakkara, A.; Challacombe, M.; Gill, P. M. W.; Johnson, B.; Chen, W.; Wong, M. W.; Gonzalez, C.; Pople, J. A. *Gaussian 03*, revision C.02; Gaussian, Inc.: Wallingford, CT, 2004.
- (21) Wakatsuki, Y. *J. Organomet. Chem.* **2004**, *689*, 4092.
- (22) Schuster, O.; Liao, R.-Y.; Schier, A.; Schmidt, H. *Inorg. Chim. Acta* **2005**, *358*, 1429.
- (23) Bilic, A.; Reimers, J. R.; Hush, N. S. *J. Chem. Phys.* **2005**, *122*, 094708.
- (24) Peterson, K. A.; Dunning, T. H., Jr. *J. Chem. Phys.* **1997**, *106*, 4119.
- (25) Lin, S.-Y.; Tsai, Y.-T.; Chen, C.-C.; Lin, C.-M.; Chen, C.-H. *J. Phys. Chem. B* **2004**, *108*, 2134.
- (26) Norman, T. J.; Grant, C. D.; Magana, D.; Zhang, J. Z.; Liu, J.; Cao, D.; Bridges, F.; Van Buuren, A. *J. Phys. Chem. B* **2002**, *106*, 7005.
- (27) Zhan, C. G.; Dixon, D. A. *J. Phys. Chem. A* **2001**, *105*, 11534.
- (28) Tuttle, T. R.; Malaxos, S.; Coe, V. C. *J. Phys. Chem. A* **2002**, *106*, 925.
- (29) Dance, I. Interactions: Theory and Scope. In *Encyclopedia of Supramolecular Chemistry*; Atwood, J. L., Steed, J. W., Eds.; Dekker: New York, 2004; p 1076.
- (30) Chang, S.-C.; Chao, I.; Tao, Y.-T. *J. Am. Chem. Soc.* **1994**, *116*, 6792.
- (31) Weiss, H.-C.; Blaser, D.; Boese, R.; Doughan, B. M.; Haley, M. M. *Chem. Commun.* **1997**, 1703.